

Exploring metal-driven stereoselectivity of glycopeptides by free-energy calculations*

Adriana Pietropaolo

*Dipartimento di Scienze della Salute, Università Magna Graecia di Catanzaro,
Viale Europa, 88100 Catanzaro, Italy*

Abstract: A formalism to quantify the chemical stereoselectivity, based on free energy of binding calculations, is here discussed. It is used to explain the stereoselectivity of two diastereoisomeric frameworks, comprising the dimer of a copper(II)-peptide core of L- and D-carnosine, respectively, each bound to two chains of D-trehalose, in which copper(II) adopts a type-II coordination geometry. The stereocenter of carnosine is varied both L and D, giving rise to two diastereoisomers. A thermodynamic cycle crossing the formation of the two enantiomeric copper(II) peptide cores was devised. A harmonic restraining potential that depends only on the bond distance was added to ensure reversibility in bond formation and dissociation, for an accurate estimate of the free energy. The calculation of the free energy of binding between D-trehalose and the two enantiomeric copper(II) peptide cores reproduces the free-energy quantities observed from stability constants and isothermal titration calorimetry (ITC) measurements. This is an example of chirality selection based on free-energy difference.

Keywords: chirality; copper; dynamics; metal complexes; molecular dynamics (MD); selection.

INTRODUCTION

Stereochemical selectivity is widely used by nature to control and regulate subtle biochemical events [1,2]. Experimentalists, as well as theoreticians, have expended a great deal of effort in attempting to understand why nature selects a defined chirality in biomolecules. For instance, it is a continuous matter of debate why natural glycans are found in the D-form, while amino acids are almost exclusively observed in the L-form. Only in the cell wall of some microorganisms [3] and various aged human tissues (tooth, bone, brain and others) [4] are D-amino acids observed.

In particular, glycan–peptide interactions require a specific stereochemistry in order to carry out their functions [5,6]. Glycopeptides have keynote functions including the regulation of cellular immune responses [7]. In their cellular compartment, proteins face a glycosidic environment, and, owing to their size, glycans can shield large regions of the protein surfaces, regulating nonspecific lateral protein–protein interactions. Furthermore, glycans lying close to the cell membrane can determine the orientation of the binding faces of the proteins to which they are attached [8–10].

As stereocenter chirality is opposite passing from glycans to proteins, it can be interesting to study the specific interactions that can be generated in a glycopeptide scaffold. In these regards, transition metals are very useful for selecting a given stereochemistry [11–14], thereby enhancing the stabil-

Pure Appl. Chem.* **84, 1837–1937 (2012). A collection of invited papers based on presentations on the Chemistry of Life theme at the 43rd IUPAC Congress, San Juan, Puerto Rico, 30 July–7 August 2011.

ity of one of the stereoisomers. Metals promote the formation of nuanced conformations by specific intramolecular interactions [15–17]. Those can be discriminated in their free-energy levels.

The phenomenological aspects of stereoselectivity can be extracted using computer simulations by calculating free energy. From this quantity we can begin to understand the chemical driving forces that underlie these complex, stereoselective processes.

When measuring stability constants or the energy quantities associated with a given process, the interesting, reactive processes take place in equilibrium conditions. It follows that the observed events have to span several times the two states under examination. For instance, in methods such as metadynamics [18], the presence of barriers in the transverse degrees of freedom leads to incomplete sampling. Ensuring reversibility is therefore crucial in order to reproduce the experimental conditions.

Among the enhanced sampling techniques [19] based on the introduction of a bias potential, metadynamics [18] has been proven to be extremely effective in studying a variety of biological processes [20–24]. Proposed as a method to sample rare events [25–30], metadynamics accurately reconstructs the free-energy landscape along specific collective variables, so-called (CVs). Those represent the reaction coordinates of the process under investigation. A recent variant of metadynamics is well-tempered metadynamics [31], in which the free-energy valleys are filled by a bias potential, whose local strength decreases with the time already spent there. This ensures free energy to converge.

A method that is able to reproduce the observed stereoselectivity of two diastereoisomers is here discussed. The former is based on well-tempered metadynamics calculations. The observed stereoselectivity is driven by a square planar coordination of copper(II) with a glycopeptide scaffold (Fig. 1, top). The dimeric copper(II) complexes with D-trehalose–L-carnosine (TrLCar) and D-trehalose–D-carnosine (TrDCar) were considered since it is a recent case of stereoselectivity observed in a metal-glycopeptide scaffold. These two diastereoisomers have different affinity for copper(II) ($\log^L - \log^D = 3.6$), which was further observed by isothermal titration calorimetry (ITC), UV and CD spectroscopy [16].

We can visualize the two diastereoisomeric frameworks as a dimer of copper(II)-peptide core of L-carnosine and of D-carnosine, each bound to two chains of D-trehalose (Fig. 1, top), in which the copper(II) coordination parameters were obtained using a combined quantum-classical QM/MM approach.

Determinant for the free-energy difference estimate is to write down a thermodynamic cycle involving the formation of the copper(II) peptide cores of L- and D-carnosine (Fig. 1, bottom). Since they are enantiomers, they have the same free-energy levels. Therefore, an accurate free-energy difference estimate derives from the calculation of the free energy of binding between D-trehalose and the copper(II) peptide cores of L- and D-carnosine. In order to observe bond formation and dissociation, a harmonic restraining potential, which depends only on the bond distance, was added. That ensures reversibility for an accurate estimate of the free energy.

The calculated free-energy difference of the two diastereoisomers by means of metadynamics reproduces the stereoselectivity quantified by ITC and stability constants measurements [16].

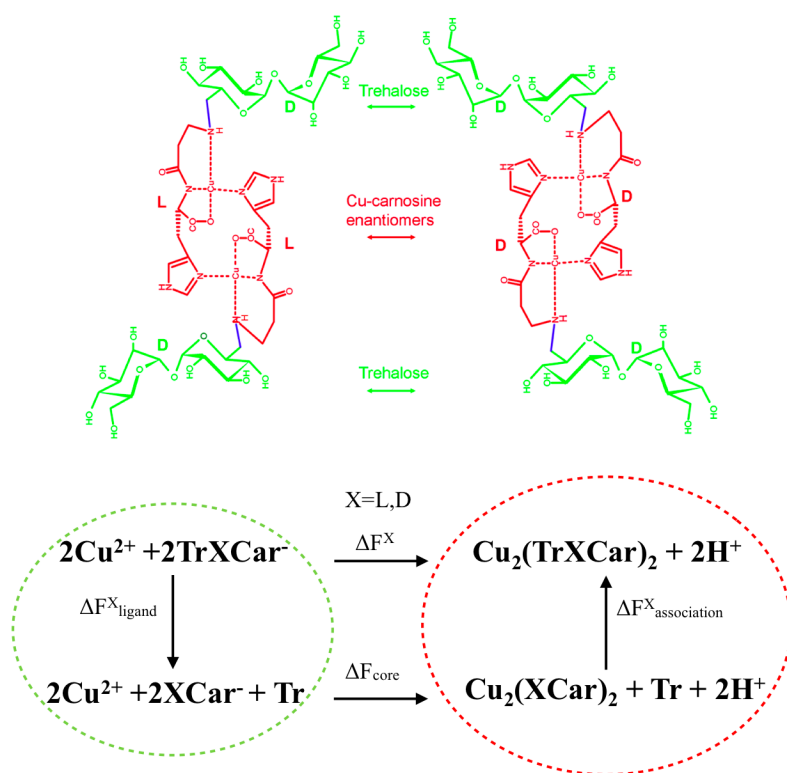


Fig. 1 (top) Representation of the diastereoisomeric frameworks of trehalose-L-carnosine and trehalose-D-carnosine copper(II) dimers. The copper(II) peptide core and the trehalose units are highlighted, as well as the trehalose–carnosine bond distance, used as CV. (bottom) Thermodynamic cycle used to calculate the free-energy differences between the two diastereoisomers. That involves the formation of the copper(II) peptide cores, whose free energies are chirality independent.

BACKGROUND

Before introducing the computational approach, a brief survey of established techniques for dealing with the free-energy calculation follows.

In recent years, impressive advances in the calculation of free energy have been achieved [19]. This comes out since the comprehension of the majority of chemical processes can be reached by examining their free-energy behavior.

Perturbation theory [32] is one of the oldest and most used methods. The main idea behind it is that given a starting initial state, so-called unperturbed or reference state, the property of the state of interest is represented by a perturbation of the reference state. Perturbation theory is commonly used to estimate free energy within the free-energy perturbation (FEP) calculations [33,34]. FEP can be applied to study protein–ligand interactions, as well as in calculating the binding free-energy difference between a bound state and an unbound state. This FEP framework is usually known as alchemical transformation calculations [19], in the sense that a chemical system through a mild alteration of it can be converted into another one. In order to reach initial and final states, intermediate states are often used. This strategy permits a reliable estimation of the free energy that can be practically done by using an ensemble of bespoke coupling parameters, usually called λ -parameters. These parameters have the function to connect the initial and final states along the reaction coordinates of the free-energy path, and

an efficient development is the λ -dynamics methodology [35], among other improvements in drug design [36].

Another general approach to estimate free energy is based on the so-called thermodynamic integration [37]. This methodology relies on calculating and thereby integrating the derivative of the free energy with respect to one or more order parameters. Also in this case, the interval of calculation is split in more sub-intervals in order to have a more accurate free-energy estimate. This is often crucial for the investigation of transition states, where the free energy is maximum, causing a very poor sampling in transition-state regions. Moreover, in each sub-interval, an extra-potential can be added in order to improve the sampling, as proposed in the umbrella sampling methodology [38]. The problem of high free-energy barriers is crucial in this type of calculation, since the free-energy estimate succeeds only if the calculated process is reversible [19,39,40]. The presence of high free-energy barriers causes an inefficient and incorrect sampling, hampering the reversibility of the process.

This problem becomes particularly important in the exploration of the free energy of bond formation in the course of molecular dynamics (MD) simulations. That arises from the difficulty in treating bond dissociation and formation in a reversible manner using classical MD studies. In addition, long-time motions are hardly accessible through MD, owing to a prohibitive computational time that hampers the efficiency of the sampling in the bound and unbound states. Several successful techniques [19] have been developed through the years in order to overcome these problems, and among those, metadynamics [18,31] can be successfully used to reconstruct the free-energy landscape along a defined CV.

A THERMODYNAMIC CYCLE TO QUANTIFY STEREOSELECTIVITY

The two molecular frameworks are shown in Fig. 1 (top). Those are constituted by a dimer of copper(II) coordinated in a type II distorted square planar environment to D-trehalose–L-carnosine and D-trehalose–D-carnosine. The coordination environment is the same in the two diastereoisomers. That involves the backbone amide, the carboxylate, the amine group and the imidazole of histidine. All of them belong to the carnosine dipeptide, whose C_{α} stereocenter is altered from L to D.

Consequently, the two copper(II) peptide cores are enantiomers and have the same free-energy levels. A thermodynamic cycle crossing the formation of the two cores of copper(II)-L-carnosine and copper(II)-D-carnosine [$Cu_2(XCar)_2$, where X is L or D] notably simplifies the calculation of the free-energy difference estimate. That is reported in Fig. 1 (bottom).

In the former cycle, we can first separate the trehalose from the carnosine, which results in the free energy of ligand formation $\Delta F_{\text{ligand}}^X$. The two free carnosines are then assembled to form the core $Cu_2(XCar)_2$. This step is obviously independent of the chirality and leads to the free energy ΔF_{core} . Then, the all complex is reassembled by adding the trehalose to the copper(II) peptide core. This last step is clearly chirality-dependent and is related to the term $\Delta F_{\text{association}}^X$. We shall assume that within the error of calculation $\Delta F_{\text{ligand}}^X$ is negligible, as shown in Fig. 2 and focus on the evaluation of $\Delta F_{\text{association}}^X$. The quantification of the chemical stereoselectivity of these two diastereoisomers therefore requires only one free-energy term, whose derivation is explained in the next section.

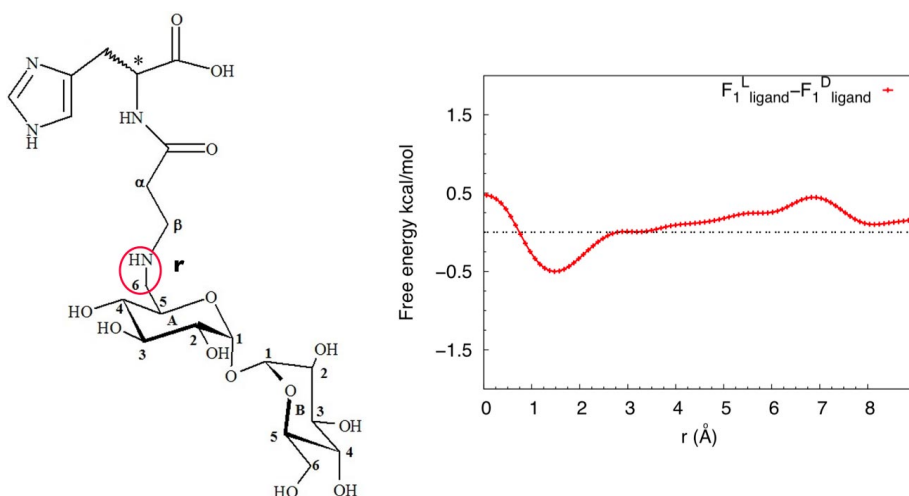


Fig. 2 Binding free-energy difference between trehalose and L/D-carnosine. The values approaching zero indicate a low free-energy contribution in the stereoselectivity observed for the two diastereoisomers.

A METHOD FOR ENSURING BINDING REVERSIBILITY

For the sake of simplicity, let us consider the case of a single collective variable, s . The free energy $F(s)$ as a function of this variable is given by eq. 1:

$$F(s) = -\frac{1}{\beta} \ln \frac{\int \delta(s - s(\mathbf{r})) e^{-\beta V(\mathbf{r})} d\mathbf{r}}{Z} \quad (1)$$

where $Z = \int e^{-\beta V(\mathbf{r})} d\mathbf{r}$, $V(\mathbf{r})$ is the interaction potential, and \mathbf{r} the atomic coordinates.

We now add to $V(\mathbf{r})$ a harmonic restraining potential that depends only on the collective coordinates, $\frac{1}{2}k(s(\mathbf{r}) - s_0)^2$. We define $F^B(s)$ as the free energy surface for the modified potential $V(\mathbf{r}) + \frac{1}{2}k(s(\mathbf{r}) - s_0)^2$ given by eq. 2:

$$F^B(s) = -\frac{1}{\beta} \ln \frac{\int \delta(s - s(\mathbf{r})) e^{-\beta(V(\mathbf{r}) + \frac{1}{2}k(s(\mathbf{r}) - s_0)^2)} d\mathbf{r}}{\int e^{-\beta(\frac{1}{2}k(s(\mathbf{r}) - s_0)^2 + V(\mathbf{r}))} d\mathbf{r}} \quad (2)$$

It is then straightforward to show that $F^B(s)$ is related to $F(s)$ by the eqs. 3 and 4:

$$F^B(s) = \frac{1}{2}k(s - s_0)^2 + F(s) + c \quad (3)$$

where c is

$$c = -\frac{1}{\beta} \ln \frac{\int ds e^{-\beta F(s)} e^{-\beta \frac{1}{2}k(s - s_0)^2}}{\int ds e^{-\beta F(s)}} \quad (4)$$

In our case, we have two collective variables, namely, the lengths of the two trehalose–carnosine bonds, and this relation will be generalized to eqs. 5 and 6:

$$F_{\lambda}^L(s_1, s_2) = \frac{\lambda}{2} K(s_1 - s_0)^2 + \frac{\lambda}{2} K(s_2 - s_0)^2 + F_0^L(s_1, s_2) + c_0^L + c_{\lambda}^L \quad (5)$$

$$F_{\lambda}^D(s_1, s_2) = \frac{\lambda}{2} K(s_1 - s_0)^2 + \frac{\lambda}{2} K(s_2 - s_0)^2 + F_0^D(s_1, s_2) + c_0^D + c_{\lambda}^D$$

$$\text{with } c_{\lambda} = \frac{1}{\beta} \ln \frac{\int ds_1 ds_2 e^{-\beta F_0^L(s_1, s_2)} e^{-\beta \frac{\lambda}{2} K(s_1 - s_0)^2} e^{-\beta \frac{\lambda}{2} K(s_2 - s_0)^2}}{\int ds_1 ds_2 e^{-\beta F_0^L(s_1, s_2)}} \quad (6)$$

The K is chosen to be the harmonic constant of the trehalose–carnosine bond and for $\lambda = 1$, it is in the bonded situation [$\text{Cu}_2(\text{TrXCar})_2$], while for $\lambda = 0$ we are in the dissociated case. The remarkable property is that in theory with a single calculation one can obtain at the same time the free energy of these two states. In practice, to evaluate $F(s)$ we shall choose an intermediate value of λ such that the restraining force is strong enough to bring back the trehalose to the carnosine, yet weak enough for the trehalose to explore regions of configuration space in which the system is fully dissociated. We have found that these conditions are satisfied for value of $\lambda = 10^{-3}$ ($\lambda K = 0.32 \text{ kcal mol}^{-1} \text{ \AA}^{-2}$), which allows s to reach distances of 6 Å where the free energy becomes flat, indicating complete dissociation. Since in this limit any dependence on the trehalose chirality is lost, we can equate the quantities according to eq. 7, thus aligning the two surfaces.

$$F_{0_{\infty}}^L(s_1, s_2) + c_0^L = F_{0_{\infty}}^D(s_1, s_2) + c_0^D \quad (7)$$

$$\Delta(c_0) = c_0^L - c_0^D = F_{0_{\infty}}^D(s_1, s_2) - F_{0_{\infty}}^L(s_1, s_2)$$

Once the free-energy surfaces at this value of λ are obtained, we can determine the free-energy difference at $\lambda = 1$, $F_1^L - F_1^D$.

As shown in Fig. 3, the two bond distances (r_1, r_2) explore bound states, identified by bond length values (typically 1.45 Å) and unbound states, identified by values far away from the bond distance. The high values of the bond distances ensure the enantiomerism of the two unbound states, since any kind of interaction between the metal peptide core and the trehalose chains is negligible.

The experimentally observed quantity is the formation free energy in the process ΔF^X . This can be calculated as a result of the cycle in Fig. 1 (bottom). As shown in the next section, the estimate of $\Delta F_{\text{association}}^X$ for the L- and D-dimers quantifies the observed stereoselectivity by means of ITC and stability constants measurements.

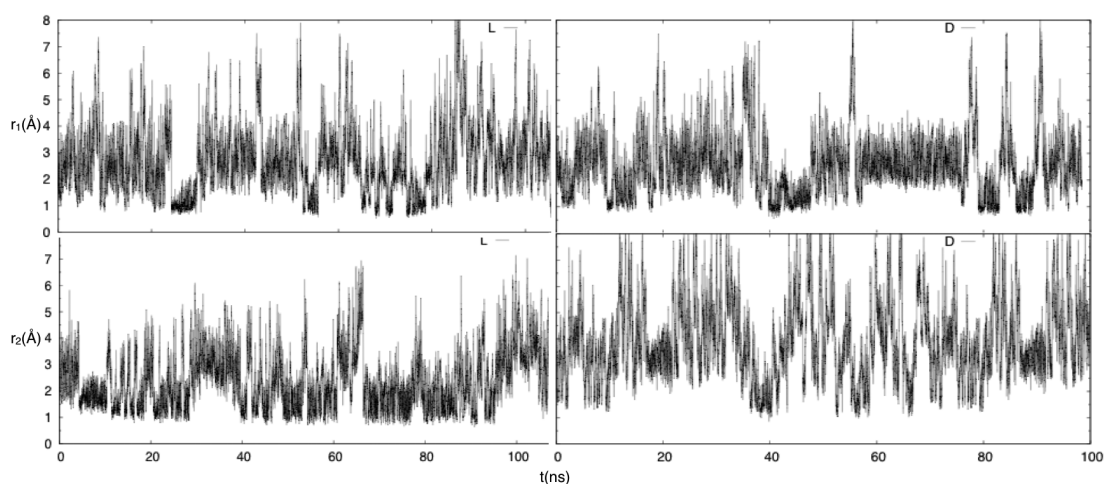


Fig. 3 Time evolution of the bond distance in the two sides of the dimer indicated by r_1 and r_2 . The two bond distances explore bound states, identified by bond length values (typically 1.45 Å) and unbound states, identified by values far away from the bond distance. The high values of the bond distances ensure the enantiomerism of the unbound states.

THE CHEMICAL FEATURES DRIVING THE STEREOSELECTIVITY

Potentiometric and calorimetric measurements show that copper(II) dimer of D-trehalose–L-carnosine is more stable than the D-trehalose–D-carnosine diastereoisomeric copper(II) dimer. Both stability constants ($\log\beta^L - \log\beta^D = 3.6$) and ΔG° values ($\Delta G^{\circ L} = -12.0$ kcal/mol, $\Delta G^{\circ D} = -7.1$ kcal/mol), as well as ΔH° ($\Delta H^{\circ L} = -6.0$ kcal/mol, $\Delta H^{\circ D} = -3.4$ kcal/mol) and ΔS° values ($\Delta S^{\circ L} = 20.0$ cal/mol, $\Delta S^{\circ D} = 13$ cal/mol) clearly state the stereoselectivity of these frameworks [16].

The difference between the two binding free energy isosurfaces, reported in Fig. 4, fully reproduce these experimental data. From the former, the L-dimer is more stable of 5 kcal/mol than the D-one. It follows that the state with $\lambda = 1$ is more stable in the L-dimer. This comes out from the higher percentage of hydrogen bonds with respect to the D-one (Fig. 5) and, interestingly, in both cases two conformations are more likely. Intriguingly, the L-dimer is much more stabilized from the D-one from CH- π interactions. Those involve the π -rich imidazole and the α -glucose rings. Moreover, two families of conformations are found. The most populated one is featured by an antiparallel orientation of the two chains. A set of conformations featured by an intra-chain hydrogen bond between the hydroxyl groups of two different chains (Fig. 5) are responsible for a parallel orientation of the chains. The former intramolecular interactions occur only in the L-dimer, thus lowering its free-energy level with respect to the D-diastereoisomer.

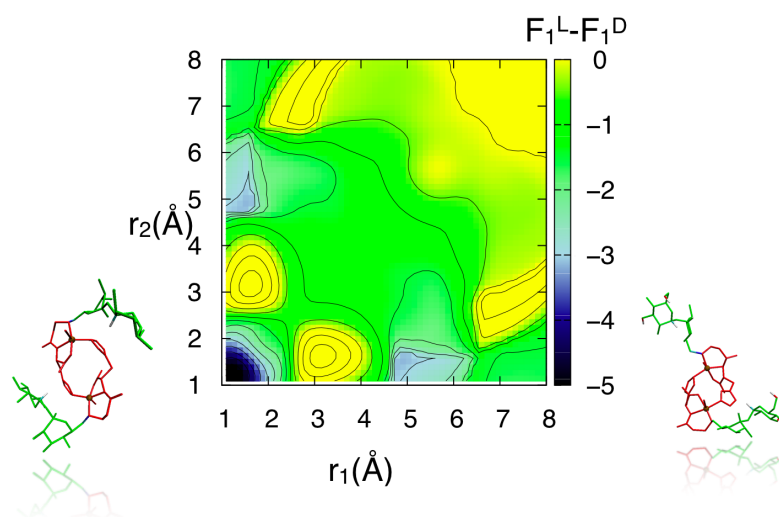


Fig. 4 Free-energy difference isosurface at $\lambda = 1$ of the two diastereoisomers, $F_1^L - F_1^D$. The L-dimer is more stable at 5 kcal/mol, as indicated by the strong minimum centered at the bond length. The isolines were drawn using a 0.5 kcal/mol spacing, and the energy panel is in kcal/mol.

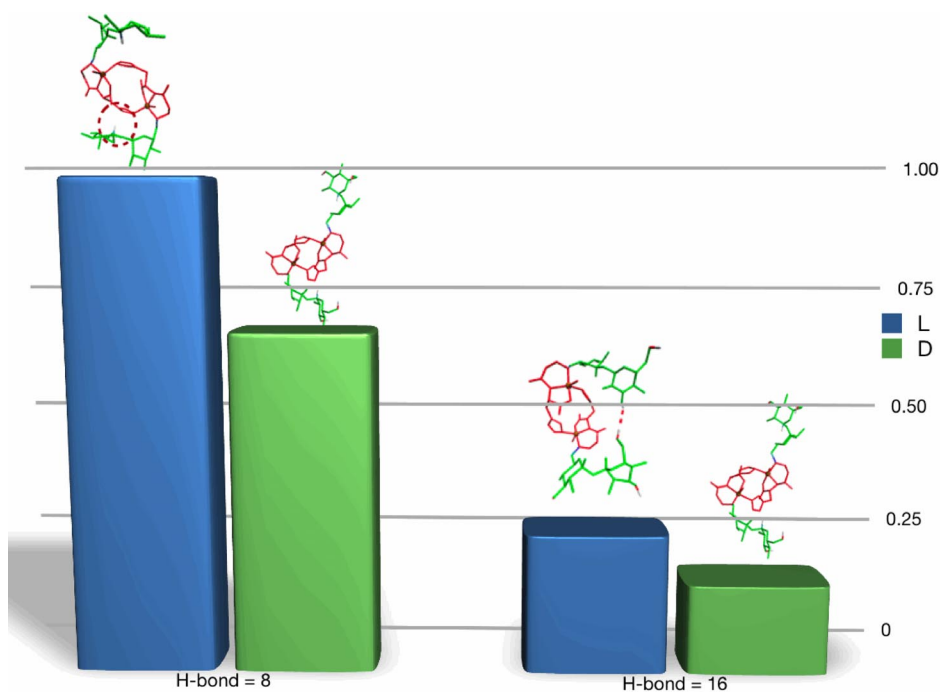


Fig. 5 Hydrogen bond (H-bond) distributions for the L- and D-dimers. The L-dimer shows a higher percentage of hydrogen bonds. Those are further stabilized by CH- π interactions, highlighted by a dashed circle, and intramolecular hydrogen bonds, indicated by a dashed line in the snapshot. Those are absent in the D-dimer. The representative conformations of the L- and D-diastereoisomers are also shown.

CONCLUSIONS

A method to explore the chemical stereoselectivity based on the calculation of the free energy of binding is here presented. We consider two diastereoisomeric copper(II) dimers of TrLCar and TrDCar. Those can be visualized as two dimers built by a copper(II)-peptide core of L-carnosine and D-carnosine each bound to two chains of D-trehalose. The two C_{α} stereocenters belonging to the peptide units are altered both L and D. The key in finding the observed free-energy differences lays in the fact that the two copper(II) peptide cores are enantiomers. The bond of D-trehalose to the enantiomeric cores leads to the chirality selection. A thermodynamic cycle involving the formation of the two enantiomeric copper(II) cores was used. Calculating the binding free-energy difference between the two diastereoisomers quantifies the observed stereoselectivity. The reversibility in the binding event was accurately ensured by including a harmonic restraining potential that depends only on the bond distance. That permits us to explore bound and unbound states.

The calculated free-energy difference is 5 kcal/mol more favorable for the L-dia stereoisomer. The free-energy estimate reproduces the stereoselectivity recently observed by means of ITC and stability constants measurements. The reason this chemical stereoselectivity is more favorable for the L-dia stereoisomer depends on the presence of CH- π interactions and on the higher number of hydrogen bonds. Altering the peptide stereocenter chirality from L to D causes the former interactions to be lost.

METHODS

Modeling the metal core units through QM/MM simulations

The metal centers were treated within a combined quantum/classical (QM/MM) approach as implemented in the ab initio software suite CP2K [41]. The X-ray structure of the copper(II) dimer with L-carnosine [42], $Cu_2(LCar)_2$, was considered as starting coordinate for the QM/MM simulation. Density functional theory (DFT) was used for the QM part $Cu_2(LCar)_2$, with the QUICKSTEP package within CP2K. A mixed Gaussian plane wave approach, suitable for large systems [43], was adopted. Perdew–Burke–Ernzerhof (PBE) [44] was used as exchange-correlation functional, with Gaussian valence basis sets of double-zeta (DZV) for hydrogen, triple-zeta with single set of polarization functions (TZVP) for nitrogen, oxygen, carbon, and copper atoms, using a spin multiplicity of singlet state, with a net charge of zero. The plane wave cutoff energy was set to 300 Ry and the norm-conserving pseudo potentials of the Goedecker, Teter, and Hutter type [45,46] were employed. A tolerance of 10^{-7} Hartree in the electronic structure was used for every time step. For the MM parts, which include only the water molecules surrounding the copper complex, TIP3P model [47] was used. A temperature of 300 K was enforced using the Nosé–Hoover thermostat [48,49]. The ESP charges used for metadynamics simulations were calculated at the HF/6-31G* level. The QM/MM coordination parameters of the copper centers are reported in Fig. 6 and are typical of a type II distorted square coordination.

Bond length (Å)	Cu ₂ (LCar) ₂
Cu–N _{amine}	1.97 ± 0.1
Cu–N _{amide}	2.10 ± 0.1
Cu–O	2.05 ± 0.1
Cu–N _{imidazole}	2.10 ± 0.1
Cu–O _{wat}	2.40 ± 0.2
Bend Angle (deg)	
N _{amine} –Cu–N _{amide}	98 ± 10
N _{amine} –Cu–O	153 ± 10
N _{amine} –Cu–N _{imidazole}	95 ± 10
N _{amide} –Cu–O	82 ± 5
N _{amide} –Cu–N _{imidazole}	145 ± 30
O–Cu–N _{imidazole}	92 ± 5
O _{wat} –Cu–N _{amine}	89 ± 10
O _{wat} –Cu–N _{amide}	107 ± 10
O _{wat} –Cu–N _{eps}	95 ± 5

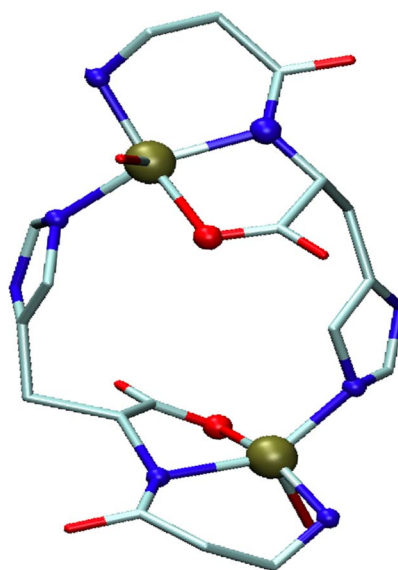


Fig. 6 Coordination geometry of the copper(II) peptide core obtained by QM/MM calculations.

Free-energy computational set-up

All MD calculations were performed by using NAMD 2.7 [50] with the Charm22 force field [51]. In order to reconstruct the free-energy surface of the copper(II) dimer of D-trehalose-L-carnosine and D-trehalose–D-carnosine, respectively Cu₂(TrLCar)₂ and Cu₂(TrDCar)₂, well-tempered metadynamics was used within the framework of PLUMED [52]. Gaussians of 0.2 kcal/mol height were deposited at 1 ps time interval, with a bias factor of 10. A temperature of 300 K was enforced using a Langevin thermostat. The QM/MM run that was used to select the starting configuration of the copper(II) peptide core as well as the copper potential parameters was used throughout the simulation. To this copper(II) peptide core, with histidine, carboxylate, and amino groups deprotonated, the trehalose chains were bound. The most representative cluster of MD conformations was selected. The D-enantiomer of the copper core, Cu₂(DCar)₂, was obtained by reflecting the QM/MM structure of Cu₂(LCar)₂ through the N_{amide}, C_α, C_β plane.

The two systems were equilibrated starting from a distance of 10 Å for 5 ns before running the simulations. Four metadynamics 100 ns long were run at low force constant value ($\lambda K = 0.32 \text{ kcal mol}^{-1} \text{ \AA}^{-2}$), for Cu₂(TrLCar)₂ and Cu₂(TrDCar)₂ and for TrLCar and TrDCar, to evaluate the binding free-energy difference estimate between trehalose and L- or D-carnosine. The two bond distances (C₆–N) between the two trehalose chains and the carnosine dipeptide were used as CVs. In order to take into account the orientation of the two trehalose chains with respect to the carnosine, the torsion θ , defined as the rotation of trehalose around the bond distance (C₅–C₆–N–C_β), was included as CV.

The CVs are taken into account in the two sides of the dimer. Finally, two metadynamics simulations 40 ns long were carried out at standard force constant ($320 \text{ kcal mol}^{-1} \text{ \AA}^{-2}$) for Cu₂(TrLCar)₂ and Cu₂(TrDCar)₂ using as CVs the θ torsion. Glycopeptide labels are reported in Fig. 2.

ACKNOWLEDGMENTS

Prof. Michele Parrinello and Prof. Enrico Rizzarelli are gratefully acknowledged for precious suggestions and discussions. Dr. Gareth Tribello and Dr. Francesco Mauriello are also acknowledged for use-

ful suggestions and critical reading of the manuscript. ETHZ Brutus cluster and CINECA are acknowledged for the computational time provided.

REFERENCES

1. H. D. Ly, S. G. Withers. *Annu. Rev. Biochem.* **68**, 487 (1999).
2. L. G. Barrientos, A. M. Gronenborn. *Mini. Rev. Med. Chem.* **5**, 21 (2005).
3. J. Corrigan. *Science* **164**, 142 (1969).
4. N. Fujii. *Orig. Life Evol. Biosphere* **32**, 103 (2002).
5. P. G. Hitchen, K. Twigger, E. Valiente, R. H. Langdon, B. W. Wren, A. Dell. *Biochem. Soc. Trans.* **38**, 1307 (2010).
6. K. Mariño, J. Bones, J. J. Kattla, P. M. Rudd. *Nat. Chem. Biol.* **6**, 713 (2010).
7. P. M. Rudd, T. Elliott, P. Cresswell, I. A. Wilson, R. A. Dwek. *Science* **291**, 2370 (2001).
8. R. G. Spiro. *Glycobiology* **12**, 43R (2002).
9. Y. C. Lee. *FASEB J.* **6**, 3193 (1992).
10. N. E. Fahmi, L. Dedkova, B. Wang, S. Golovine, S. M. Hecht. *J. Am. Chem. Soc.* **129**, 3586 (2007).
11. Q. Ma, Z. Xu, B. R. Schroeder, W. Sun, F. Wei, S. Hashimoto, K. Konishi, C. J. Leitheiser, S. M. Hecht. *J. Am. Chem. Soc.* **129**, 12439 (2007).
12. R. M. Hazen, D. S. Sholl. *Nat. Mater.* **2**, 367 (2003).
13. X. Huang, K. Nakanishi, N. Berova. *Chirality* **12**, 237 (2000).
14. R. Lauceri, A. Raudino, L. M. Scolaro, N. Micali, R. Purrello. *J. Am. Chem. Soc.* **124**, 894 (2002).
15. A. H. Hoveyda, P. J. Lombardi, R. V. O'Brien, A. R. Zhugralin. *J. Am. Chem. Soc.* **131**, 8378 (2009).
16. G. I. Grasso, G. Arena, F. Bellia, G. Maccarrone, M. Parrinello, A. Pietropaolo, G. Vecchio, E. Rizzarelli. *Chem.—Eur. J.* **17**, 9448 (2011).
17. F. Bellia, D. La Mendola, C. Pedone, E. Rizzarelli, M. Saviano, G. Vecchio. *Chem. Soc. Rev.* **38**, 2756 (2009).
18. A. Laio, M. Parrinello. *Proc. Natl. Acad. Sci. USA* **99**, 12562 (2002).
19. C. Chipot, A. Pohorille. *Free Energy Calculations: Theory and Applications in Chemistry and Biology*, Springer, Berlin (2007).
20. A. Pietropaolo, D. Branduardi, M. Bonomi, M. Parrinello. *J. Comput. Chem.* **32**, 2627 (2011).
21. J. Pfaendtner, D. Branduardi, M. Parrinello, T. D. Pollard, G. A. Voth. *Proc. Natl. Acad. Sci. USA* **106**, 12723 (2009).
22. A. Barducci, M. Bonomi, M. Parrinello. *Wiley Interdisc. Rev.: Comput. Mol. Sci.* **1**, 826 (2011).
23. D. Branduardi, F. L. Gervasio, A. Cavalli, M. Recanatini, M. Parrinello. *J. Am. Chem. Soc.* **127**, 9147 (2005).
24. M. Bonomi, M. Parrinello. *Phys. Rev. Lett.* **104**, 190601 (2010).
25. X. Daura, W. F. Van Gunsteren, A. E. Mark. *Angew. Chem., Int. Ed.* **34**, 269 (1999).
26. W. F. van Gunsteren, D. Bakowies, R. Baron, I. Chandrasekhar, M. Christen, X. Daura, P. Gee, D. P. Geerke, A. Glättli, P. H. Hünenberger, M. A. Kastenzholz, C. Oostenbrink, M. Schenk, D. Trzesniak, N. F. van der Vegt, H. B. Yu. *Angew. Chem., Int. Ed.* **45**, 4064 (2006).
27. H. Grubmüller. *Phys. Rev. E* **52**, 2893 (1995).
28. H. Grubmüller, B. Heymann, P. Tavan. *Science* **271**, 997 (1996).
29. G. A. Tribello, M. Ceriotti, M. Parrinello. *Proc. Natl. Acad. Sci. USA* **107**, 17509 (2010).
30. M. Ceriotti, G. A. Tribello, M. Parrinello. *Proc. Natl. Acad. Sci. USA* **108**, 13023 (2011).
31. A. Barducci, G. Bussi, M. Parrinello. *Phys. Rev. Lett.* **100**, 020603 (2008).
32. J. G. Kirkwood. *J. Chem. Phys.* **3**, 300 (1935).
33. J. L. Knight, C. L. Brooks III. *J. Comput. Chem.* **30**, 1692 (2009).
34. W. L. Jorgensen, L. L. Thomas. *J. Chem. Theory Comput.* **4**, 869 (2008).

35. X. Kong, C. L. Brooks III. *J. Chem. Phys.* **105**, 2414 (1996).
36. J. Aqvist, C. Medina, J. E. Samuelsson. *Protein Eng.* **7**, 385 (1994).
37. M. Sprik, G. Ciccotti. *J. Chem. Phys.* **109**, 7737 (1998).
38. J. N. Patey, J. P. Valleau. *J. Chem. Phys.* **63**, 2334 (1975).
39. M. Parrinello. In *Physical Biology from Atoms to Medicine*, A. H. Zewail (Ed.), pp. 247–265, Imperial College Press, London (2008).
40. V. Leone, F. Marinelli, P. Carloni, M. Parrinello. *Curr. Opin. Struct. Biol.* **20**, 148 (2010).
41. J. VandeVondele, M. Krack, F. Mohamed, M. Parrinello, T. Chassaing, J. Hutter. *Comput. Phys. Commun.* **167**, 103 (2005).
42. H. C. Freeman, J. T. Szymanski. *Acta Crystallogr.* **22**, 406 (1967).
43. G. Lippert, J. Hutter, M. Parrinello. *Mol. Phys.* **92**, 477 (1997).
44. J. P. Perdew, K. Burke, M. Ernzerhof. *Phys. Rev. Lett.* **77**, 3865 (1996).
45. S. Goedecker, M. Teter, J. Hutter. *Phys. Rev. B: Condens. Matter* **54**, 1703 (1996).
46. C. Hartwigsen, S. Goedecker, J. Hutter. *Phys. Rev. B: Condens. Matter* **58**, 3641 (1998).
47. W. L. Jorgensen. *J. Am. Chem. Soc.* **103**, 335 (1981).
48. W. G. Hoover. *Phys. Rev. A* **31**, 1695 (1985).
49. S. Nosé. *Mol. Phys.* **52**, 255 (1984).
50. J. C. Phillips, R. Braun, W. Wang, J. Gumbart, E. Tajkhorshid, E. Villa, C. Chipot, R. D. Skeel, L. Kalé, K. Schulten. *J. Comput. Chem.* **26**, 1781 (2005).
51. A. D. MacKerell Jr., M. Feig, C. L. Brooks III. *J. Comput. Chem.* **25**, 1400 (2004).
52. M. Bonomi, D. Branduardi, G. Bussi, C. Camilloni, D. Provasi, P. Raiteri, D. Donadio, F. Marinelli, F. Pietrucci, R. A. Broglia, M. Parrinello. *Comput. Phys. Commun.* **180**, 1961 (2009).